Research paper

EARTHQUAKE SPECTRA

Earthquake Spectra
2020, Vol. 36(2) 856–879

DOI: 10.1177/8755293019891729
journals.sagepub.com/home/eqs
SAGE

Modeling nonlinear site effects in physics-based ground motion simulations of the 2010–2011 Canterbury earthquake sequence

Christopher A de la Torre, M.EERI, Brendon A Bradley, M.EERI and Robin L Lee, M.EERI

Abstract

This study examines the performance of nonlinear total stress one-dimensional (1D) wave propagation site response analysis for modeling site effects in physics-based ground motion simulations of the 2010–2011 Canterbury, New Zealand earthquake sequence. This approach explicitly models three-dimensional (3D) ground motion phenomena at the regional scale, and detailed site effects at the local scale. The approach is compared with a more commonly used empirical V_{S30}-based method of computing site amplification for simulated ground motions, as well as prediction via an empirical ground motion model. Site-specific ground response analysis is performed at 20 strong motion stations in Christchurch for 11 earthquakes with $4.7 \leqslant M_W \leqslant 7.1$. When compared with the V_{S30}-based approach, the wave propagation analysis reduces both overall model bias and uncertainty in site-to-site residuals at the fundamental period, and significantly reduces systematic residuals for soft or "atypical" sites that exhibit strong site amplification. The comparable performance in ground motion prediction between the physics-based simulation method and empirical ground motion models suggests the former is a viable approach for generating site-specific ground motions for geotechnical and structural response history analyses.

Keywords

Site effects, soil nonlinearity, site response analysis, ground motion simulation

Date received: 17 January 2019; accepted: 10 October 2019

Department of Civil and Natural Resources Engineering, University of Canterbury, Christchurch, New Zealand

Corresponding author:
Christopher A de la Torre, Department of Civil and Natural Resources Engineering, University of Canterbury, Private Bag 4800, Christchurch 8140, New Zealand.
Email: christopher.delatorre@pg.canterbury.ac.nz

Introduction

Three-dimensional (3D) physics-based ground motion simulation methods are being increasingly used to predict ground motion intensity, with accuracy and precision that rivals conventional empirical models (e.g. Bradley et al., 2017; Taborda and Bielak, 2013). Limitations associated with computation, modeled physics, and data availability often result in the use of "hybrid" simulations which involve a comprehensive solution of the 3D wave equation for low frequencies (LFs), and a simplified-physics approach for high frequencies (HFs). The transition between the LF and HF approaches varies across research efforts, but is commonly at $f = 1$ Hz (Graves and Pitarka, 2010; Razafindrakoto et al., 2016), which implies a spatial discretization in the velocity model in the order of 100 m, with additional factors being the minimum shear wave velocity, and specific numerical method adopted. In addition, the comprehensive 3D solution commonly models the 3D medium as viscoelastic, although recent attempts have also explicitly considered plasticity (Roten et al., 2016; Taborda et al., 2012), albeit without direct validation against observations and only at LFs (i.e. coarse spatial scales).

Given the sentiments above, near-surface nonlinear site effects in broadband ground motion simulations must therefore, at present, be computed separately from the regional 3D simulation. Four methods have been used or proposed to incorporate nonlinear soil response into 3D ground motion simulations: (1) fully coupled LF (i.e. coarse grid) 3D simulation models that explicitly consider soil nonlinearity in surficial soils (e.g. Restrepo et al., 2012; Taborda et al., 2012), (2) the domain reduction method for decomposing the physical domain into multiple subdomains for separate simulation (e.g. Bielak et al., 2003; Yoshimura et al., 2003), (3) conventional one-dimensional (1D) wave propagation site response analysis uncoupled from the simulations (e.g. Hartzell et al., 2002; Roten et al., 2012), and finally (4) the use of simple empirically based site amplification factors (e.g. Graves and Pitarka, 2010, 2015). The most common way to do so is via empirical V_{S30}-based site effects models (i.e. Method 4, e.g. Graves and Pitarka, 2010; Razafindrakoto et al., 2018). This empirical treatment of site effects in ground motion simulations is simple relative to the physics-based source and path modeling of simulations, and the state-of-the-art in geotechnical seismic ground response analysis (Régnier et al., 2016; Stewart et al., 2008, 2017), suggesting that there is room for improvement in how site effects are modeled in the context of simulations.

Hartzell et al. (2002) and Roten et al. (2012) are examples of where the more comprehensive physics-based 1D nonlinear wave propagation site response analysis was used for modeling site effects in ground motion simulations. These studies performed simulations of potential future earthquakes on the Seattle and Wasatch Faults, respectively, and therefore lack direct validation against observed ground motions. The nonlinear ground response was computed at hundreds of sites across the region using generalized regional subsurface data primarily based on geology, and hence soil stratification, shear wave velocity profiles, and constitutive model inputs were idealized. The results of these studies were not benchmarked against empirical site amplification functions or GMMs.

As in Hartzell et al. (2002) and Roten et al. (2012), this study also explicitly models nonlinear site response in the context of 3D regional ground motion simulations using a physics-based 1D wave propagation site response approach. It is distinct in that it analyzes 11 observed earthquakes at 20 strong motion stations (SMSs) to validate the methodology and compute statistically significant site- and event-specific bias and uncertainty. The events and sites considered are described in section "Earthquakes and sites considered." The SMSs are well-characterized geotechnically and geophysically, and therefore, detailed

and representative soil profiles are used for each site. The methodology for the alternative site response approaches is given in section "Methodology." Sections "Qualitative comparison of observed and simulated ground motions" and "Systematic prediction residuals" present results in terms of intensity measures and systematic prediction residuals. Finally, in section "Comparison with prediction from empirical GMM" the systematic performance of simulations with both site response methods is compared with prediction from a conventional empirical GMM. Supplementary tables, figures, and analysis interpretation are included in Supplemental Appendices A to E, and are referenced throughout the main body of the article accordingly.

Earthquakes and sites considered

Events from the 2010 to 2011 Canterbury earthquake sequence

Figure 1 illustrates the 11 moderate-to-large magnitude (i.e. $4.7 \leqslant M_W \leqslant 7.1$) earthquakes and 20 SMSs considered for this study, with additional date and M_W information in Table A.1 of Supplemental Appendix A. Ten of the events occurred during the 2010–2011 Canterbury, New Zealand earthquake sequence and were simulated by Razafindrakoto et al. (2016). The 11th event was the M_W5.8 Valentine's day earthquake from 2016 and was simulated by Razafindrakoto and Bradley (2016). These 11 events generated ground motions of engineering significance that may have been influenced by nonlinear soil response in Christchurch (Bradley, 2015). The largest magnitude, and most economically and environmentally destructive events were the 4 September 2010 M_W7.1 Darfield earthquake and the 22 February 2011 M_W6.2 Christchurch earthquake (Cubrinovski et al., 2011, 2014; Quigley et al., 2016; van Ballegooy et al., 2014).

In the context of kinematic rupture description, as elaborated in Razafindrakoto et al. (2016), for the four largest magnitude events (i.e. Events 1, 4, 7, and 10 in Table A.1 of Supplemental Appendix A), the geometry of the finite fault source models from Beavan et al. (2011) and Beavan et al. (2012) was used. The two M_W5.8 earthquakes (i.e. Events 9

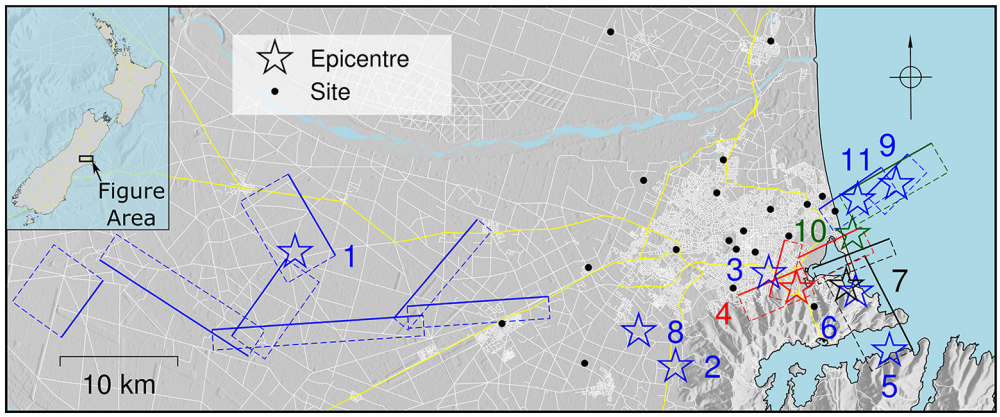

Figure 1. Illustration of simulated rupture models for 11 events, listed in Table A.1 of Supplemental Appendix A labeled by event ID, and location of 20 strong motion stations considered. Events 2, 3, 5, 6, and 8 were modeled as a point source and therefore no rupture plane is shown. The inset shows New Zealand with the vicinity of the region of this study marked by a black rectangle.

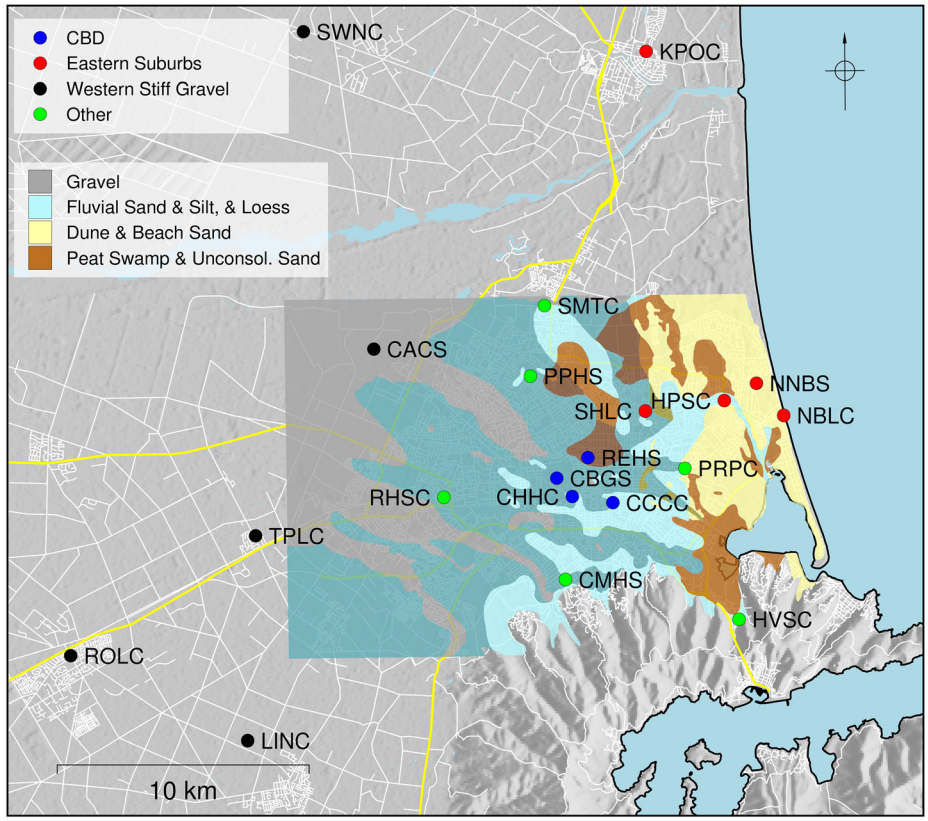

Figure 2. Location of the 20 strong motion stations analyzed in this study relative to the Christchurch urban area. Sites are grouped by geographic region and site response characteristics. Surface geology following Brown et al. (1995) is also included in the map. The darker shades of each color in the geologic descriptions indicate that gravel deposits are present at depths greater than 3 m.

and 11) used finite faults generated as a plane of appropriate along-strike length and down-dip width centered about the earthquake centroid. The remaining five events were modeled as point sources because of their small magnitudes (and therefore rupture area).

Christchurch SMS considered

To compare and validate simulated ground motions with observations, the site response analysis was performed at 20 SMSs that recorded the sequence of events. Figure 2 shows the location of sites, grouped for analysis interpretation by geographic region, site conditions, and site response characteristics into Central Business District (CBD), Eastern suburbs, Western stiff gravel, and "other sites," which do not conform to these classifications, as annotated in the figure legend. Also included in Figure 2 is surface geology by Brown et al. (1995) which is discussed in the last paragraph of this section with regards to the shear wave velocity profiles in Figure A.1 of Supplemental Appendix A.

Table A.2 in Supplemental Appendix A presents the observed geometric mean peak ground accelerations (PGAs) for the considered stations and events. The PGA values range from 0.01 to 1.36 g, with a mean PGA of 0.17 g.

Figure A.1 in Supplemental Appendix A illustrates shear wave velocity (V_S) profiles of the 20 sites based on site investigation results from Wotherspoon et al. (2014), Deschenes et al. (2018), and Jeong and Bradley (2017a). Wotherspoon et al. (2014) also performed detailed site investigations at most of the sites, including surface wave testing (using active and passive methods), cone penetration tests (CPTs), standard penetration tests (SPTs), and laboratory index tests. The velocity profiles in these studies were obtained from surface wave inversions with constant V_S values within each layer. Pressure dependence (i.e. depth dependence) was subsequently applied to the shear wave velocity of each layer in such a way as to maintain equal travel time between the published pressure-independent and pressure-dependent profiles used in this analysis. The pressure dependence is applied using the formulation of the constitutive model which is described in section "Methodology for nonlinear wave propagation site response analysis." The corresponding "profile periods" (T_1^*) of the sites in Figure A.1 in Supplemental Appendix A and the V_{S30} values used to compute empirical site amplification are given in Table A.2 of Supplemental Appendix A. T_1^* is computed as the fundamental period of the pressure independent V_S profiles above the halfspace used in the analyses (i.e. the same profiles in Figure A.1 in Supplemental Appendix A albeit without pressure dependence). Importantly, it differs from the site period which is typically defined as the period of the entire soil profile above bedrock, which is not reached in these analyses due to the great depth of the Canterbury basin ("Methodology" section should be referenced for more details on site response analysis).

In examining Figure A.1 in Supplemental Appendix A, while the near surface velocities are similar between CBD and Eastern Suburbs (about 150–200 m/s), the Eastern Suburbs profiles generally have thicker soil deposits above the stiff gravels that were used as the half space (i.e. total depths of 29–46 m compared with 20–25 m in CBD). From surface geology on Figure 2, the CBD sites are primarily fluvial sands and silts except for Resthaven (REHS) which is a peat swamp deposit. As indicated by the darker shades of the respective colors in these geologic regions, some gravels are present at depths greater than 3 m at these sites. The Eastern Suburbs sites are dune and beach sands with no gravels present at shallow depths, except for SHLC which sits on fluvial sand and silt. The Western Stiff Gravel sites all have gravel up to or near the ground surface with higher velocities, and are therefore shallower profiles (i.e. 14–20 m deep). Many of the profiles have velocity inversions (i.e. layers of lower velocity below layers of higher velocity) due to interbedded sand/gravel and silt/clay layers. This is consistent with the interbedded nature of the geology in the Canterbury basin which generally alternates between terrestrial gravel and marine sediment deposits (Lee et al., 2017b).

Methodology

Two common methods for modeling site response are adopted for the context of ground motion simulations: an empirical V_{S30}-based site amplification function, and physics-based 1D wave propagation. These two simulations that account for site effects are also compared with a reference viscoelastic simulation that neglects near-surface site effects and soil nonlinearity. The specific methodologies for all analyses are provided in the following subsections.

Reference viscoelastic condition without site response

Simulated ground motions that do not account for shallow site response are used as a reference result. As presented in Razafindrakoto et al. (2016), these are simulations performed using the Graves and Pitarka (2010) methodology without modification for site response.

To resolve the comprehensive LF component of the ground motion simulations at 1 Hz, a velocity model grid spacing of 100 m was used with a minimum shear wave velocity of 500 m/s in the simulations (Razafindrakoto et al., 2016), despite the near-surface shear wave velocities at deep sedimentary sites being lower than 500 m/s in reality. Because the simulations are viscoelastic, soil nonlinearity is not considered. In addition to these simulations being used as a reference result, they are also the "input" motions for site response analysis methods as described in the next two subsections. In figures throughout the article, this analysis is referred to as "no site response" to highlight the fact that no site effects analysis was performed.

Site effects via empirical V_{S30}-based site amplification

V_{S30}-based site amplification functions from published empirical GMMs are commonly used to compute site amplification factors that can be applied to the reference simulated ground motions (e.g. Graves and Pitarka, 2010). Figure 3a shows an example of frequency (i.e. vibration period)-dependent nonlinear site amplification factors from the empirical GMM used in this study (Campbell and Bozorgnia, 2014). This function is then truncated at short and long periods, as in Figure 3a, following recommendations by Graves and Pitarka (2010), for two different reasons. Long period (i.e. LF) site amplification is truncated because the 3D LF component of the simulation should, to some extent, account for deep site response which would influence long period ground motion amplitudes. Short periods (i.e. HFs) are truncated because empirical GMM amplification functions are developed to be applied to response spectra, but in this context they are applied to Fourier spectra in the frequency domain (Graves and Pitarka, 2010). The short period truncation is applied to partially resolve this inconsistency. Bora et al. (2016) discuss the relationship between Fourier and response spectra in the context of ground motion amplification.

Site effects via physics-based 1D wave propagation analysis

The 1D wave propagation ground response analysis enables explicit modeling of the soil stratigraphy and dynamic response at each site. As shown schematically in Figure 3b, reference viscoelastic simulated ground motions are extracted at each site considered, deconvolved, and then used as input to a nonlinear 1D site response analysis. Ground motions are extracted from the simulation at the ground surface, rather than at depth, so that 3D ground motion phenomena, such as basin effects and surface waves, are present given the subsequent use of 1D analyses to model surficial site response.

Because the regional ground motion simulations are viscoelastic, they are deconvolved in the frequency domain using a transfer function for damped soil over an elastic halfspace (e.g. Kramer, 1996) with a 1D V_S profile representative of the velocity model used for the simulation. Ground motions are deconvolved to a depth where nonlinear soil behavior is considered practically negligible. In Christchurch, this typically corresponds to the depth of the Riccarton gravels formation, with a V_S of approximately 400 m/s at depths ranging from 20 to 40 m (deepening to the east; Lee et al., 2017b; McGann et al., 2017; Wotherspoon et al., 2014). In this particular application, because the simulation grid is coarse (i.e. 100 m spacing), and the depth of deconvolution is relatively shallow (i.e. 20–40 m), the V_S profile for deconvolution is simply a single uniform layer (with $V_S = V_{S,min}$ (i.e. typically 500 m/s in Christchurch)) over a halfspace. The methodology for the nonlinear convolution (i.e. site response analysis) is described in the next subsection.

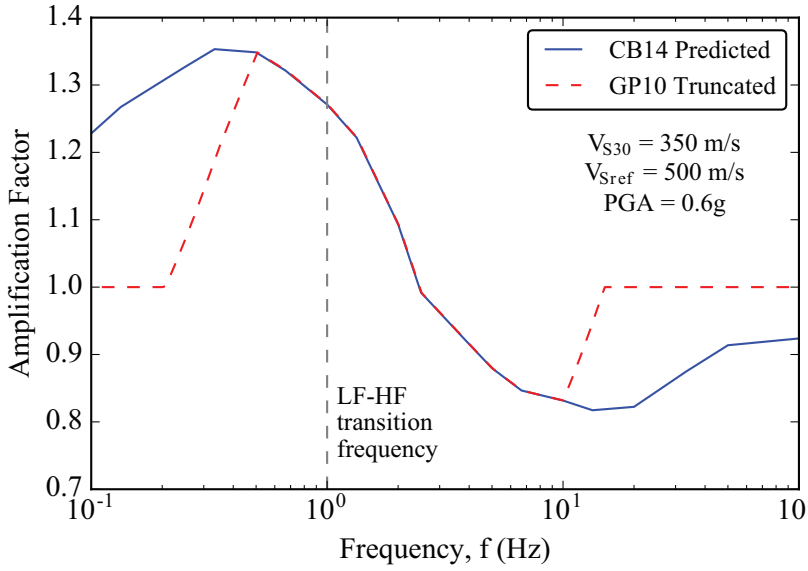

(a)

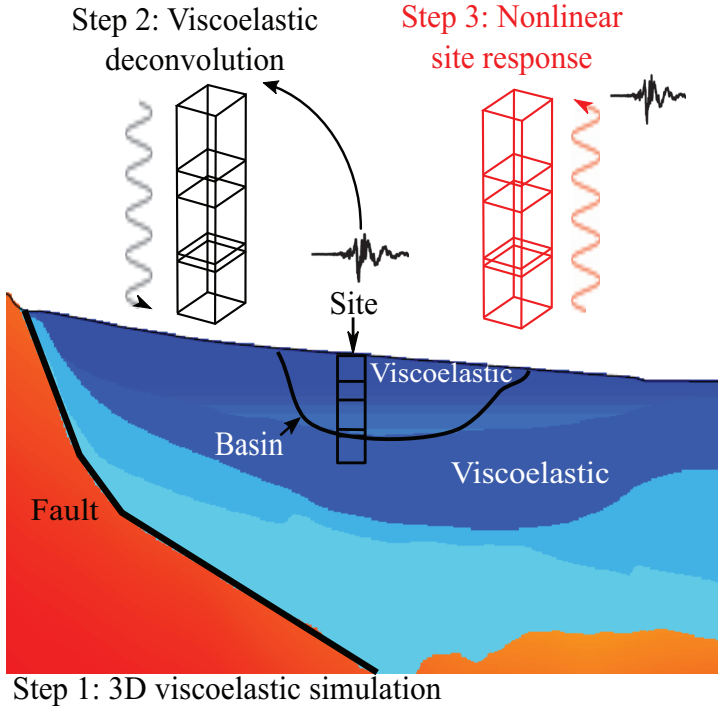

(b)

Figure 3. Two methods considered in this study for modeling nonlinear site effects in simulated ground motions: (a) Empirical V_{S30}-based nonlinear site amplification factors from Campbell and Bozorgnia (2014) (i.e. CB14) GMM truncated following Graves and Pitarka (2010) (i.e. GP10), applied to simulated ground motions in the frequency domain and (b) 1D wave propagation site response in which simulated ground motions are extracted from 3D simulation model, deconvolved, and convolved via nonlinear wave propagation site response analysis.

Methodology for nonlinear wave propagation site response analysis

Site response analyses were performed with the nonlinear finite element software OpenSees (McKenna, 2011). The 1D (i.e. vertical) shear wave propagation for a single horizontal component of ground motion was used with 2D nine-noded quadratic elements constrained to deform in horizontal shear. Geometric mean intensity measures were computed from the two simulations with each horizontal component. Elements were sized for each layer to resolve a maximum frequency of 25 Hz based on linear stiffness. The model uses a single-element-wide soil column with periodic boundary conditions on the lateral boundaries of the model, and a compliant base. The pressure-dependent multi-yield (PDMY02) constitutive model (Yang et al., 2003) was used to represent nonlinear soil behavior. The 1D site response analysis was used because of its widespread adoption in practice and research although we acknowledge the commonly stated limitations of this methodology as demonstrated through validation studies (e.g. Kaklamanos et al., 2013; Thompson et al., 2009).

CPTs in the vicinity of each site (Wotherspoon et al., 2014) were used for determining detailed stratigraphy, and the strength and relative density of each soil layer. Parameters estimated using CPT data were unit weight, friction angle, relative density, and undrained shear strength. In cases where geotechnical investigations showed the presence of interbedded softer silt layers that were not identified in the V_S profiles from surface wave inversions, a CPT-V_S correlation (McGann et al., 2017) was used to estimate the velocity of these layers. Friction angle and undrained shear strength estimates from SPT data were also used to verify and supplement CPT-based estimates.

Wotherspoon et al. (2014) performed CPT-based liquefaction triggering analysis (Robertson and Wride, 1998), and we additionally performed SPT-based liquefaction analysis (Idriss and Boulanger, 2008) to identify soils susceptible to liquefaction (for the purpose of examining subsequent analysis results). While liquefiable soils are present at some sites, the large majority of the events were not severe enough to trigger liquefaction. In this study, the hydraulic conductivity of each soil layer is set artificially high to prevent generation of pore pressure, therefore, the contraction and dilation parameters of the constitutive model have a negligible impact on the response. Future work is intended to directly examine the differences between total and effective stress analyses.

Decomposition of prediction residuals

One of the novelties of this work is the validation of simulation results against observed ground motions from multiple earthquake events and stations, enabling repeatable prediction effects to be estimated. Using similar notation as Al Atik et al. (2010) and Bradley (2015), the total prediction residual, Δ, for a given intensity measure can be expressed as

$$\Delta_{es} = ln(IM_{Obs})_{es} - ln(IM_{Sim})_{es} \quad (1)$$

where $ln(IM_{Obs})_{es}$ is the natural logarithm of the observed intensity measure for earthquake e at site s, and $ln(IM_{Sim})_{es}$ is the logarithm of the respective simulated intensity measure. The intensity measures considered in this study are 5%-damped geometric mean (from both horizontal components) response spectral accelerations at 200 vibration periods logarithmically spaced between 0.01 and 10 s.

To identify systematic trends in prediction bias for a given earthquake e, and specific site s, the prediction residual in Equation 1 can be partitioned as

$$\Delta_{es} = a + \delta S2S_s + \delta B_e + \delta W_{es}^0 \tag{2}$$

where a is the constant systematic model bias for all earthquakes and sites considered, $\delta S2S_s$ is the systematic site-to-site residual for site s, δB_e is the between-event residual for earthquake e, and δW_{es}^0 is the "remaining" within-event residual for earthquake e at site s, that is apparently random. The sum $(a + \delta S2S_s)$ is the systematic portion of the residual for a given site and is herein referred to as the systematic residual.

The between-event (δB_e), site-to-site ($\delta S2S_s$), and "remaining" within-event (δW_{es}^0) residuals are assumed to be normally distributed with zero mean and variances of τ^2, ϕ_{S2S}^2, and ϕ_{SS}^2, respectively. The total variance is then expressed as

$$\sigma^2 = \tau^2 + \phi_{S2S}^2 + \phi_{SS}^2 \tag{3}$$

For an individual site, s, the variance in the within-event residuals (i.e. $\delta W_{es} = \delta S2S_s + \delta W_{es}^0$) at that site is represented by $\phi_{SS,s}^2$. The evaluation of Equation 2 for all events and sites considered is performed using linear mixed-effects regression with the lme4 package in R (Bates et al., 2015).

Qualitative comparison of observed and simulated ground motions

To illustrate the salient features of the analyses undertaken, this section provides a qualitative summary for a subset of results, while the subsequent section provides statistical analysis of results from all sites and events. Figure 4 plots response spectra of observed and simulated ground motions from all three methods for the 4 September 2010 M_W7.1 earthquake at the HVSC site, and the 13 June 2011 M_W5.3 earthquake at the RHSC site. Also included in the figure are acceleration time series for observed ground motions and the two simulations that model nonlinear soil response. These two examples are intended to illustrate relative differences between the various methods of modeling site effects.

Comparing the simulated response spectra in Figure 4 it is evident that for $T > 5$ s all three analyses are essentially the same, suggesting the site response methods have little influence on the ground motion at long periods. Trends in response spectral accelerations seen in Figure 4, that are also generally visible across most of the data are (1) the empirical V_{S30}-based site amplification function results in greater amplification of long periods, (2) the wave propagation analysis results in greater amplification at short periods, and (3) the reference viscoelastic simulations that neglect shallow site effects greatly under-predict spectral accelerations near the profile period (0.39 and 0.29 s for HVSC and RHSC, respectively). These trends are discussed further with respect to observed-to-simulated residuals in subsequent sections.

Comparing the simulations with the observations, in both of these examples, the physics-based wave propagation method of modeling site response yields closer agreement to observations than the empirical V_{S30}-based method. Figure 4b is a good example of how there can be imprecisions in the reference or input simulations used for subsequent site response analyses as seen by the large overprediction in the reference viscoelastic

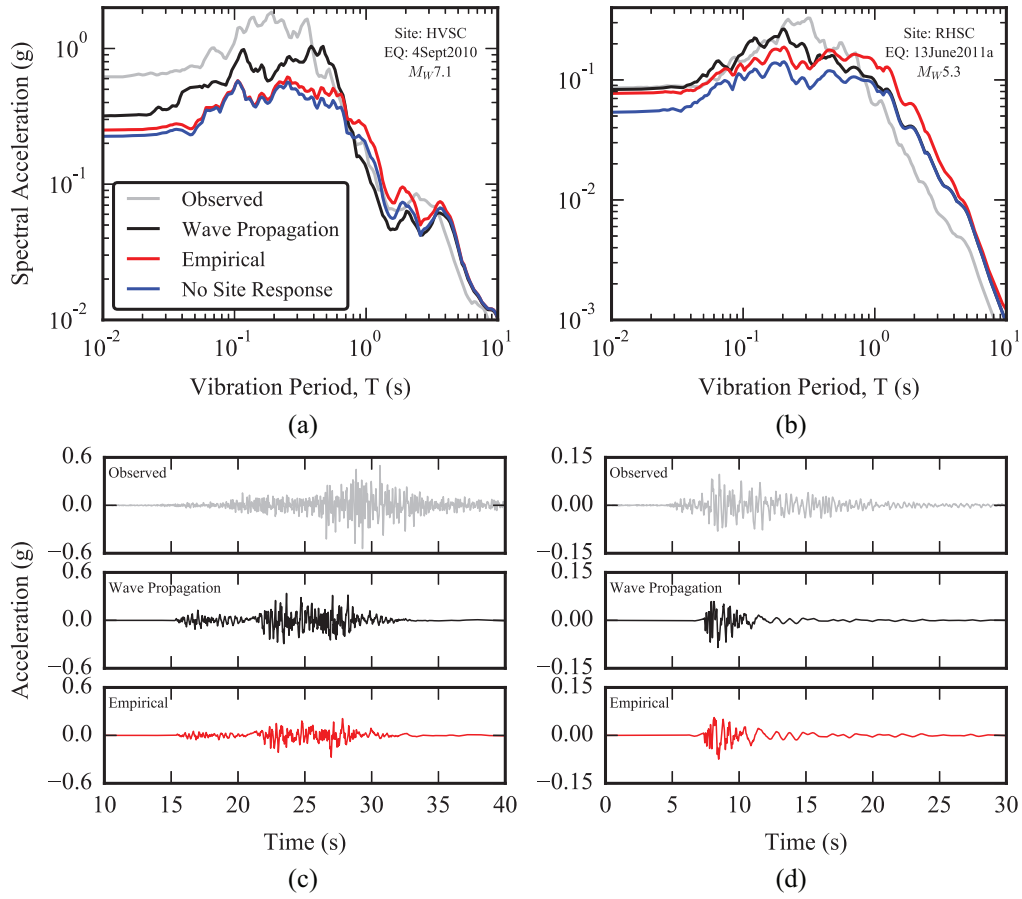

Figure 4. Comparison of 5%-damped geometric mean response spectra and acceleration time series for observed and simulated ground motions from (a and c) 4 September 2010 M_W7.1 earthquake at HVSC, and (b and d) 13 June 2011 M_W5.3 earthquake at RHSC. Note different *y*-axis scales between the left and right figures.

simulation without site response for $T > 1$ s. Such imprecisions in the input motion will manifest as imprecisions in downstream analyses as shown in Figure 4b.

In general, the simulated acceleration time series for the 4 September 2010 event (Figure 4c) are consistent with observations in terms of frequency content and duration. However, the arrival time of the strongest shaking is different, which may be caused by the complex multi-fault rupture of this event. As also seen in the response spectra, there is significant underprediction in the amplitudes of simulations which is much more prominent for the empirical V_{S30}-based method. HVSC is a site that exhibits abnormally large ground amplification, as discussed in section "Systematic residuals for individual sites." For the 13 June 2011 event (Figure 4d) the simulated acceleration time series are relatively consistent with observations in amplitude and frequency content. The duration of shaking is clearly underestimated, which is consistent with results from Lee et al. (2020) who found that the HF path duration model was too short, resulting in underestimation of significant duration for small-to-moderate magnitude events. Also, simulations of this event show late, very LF

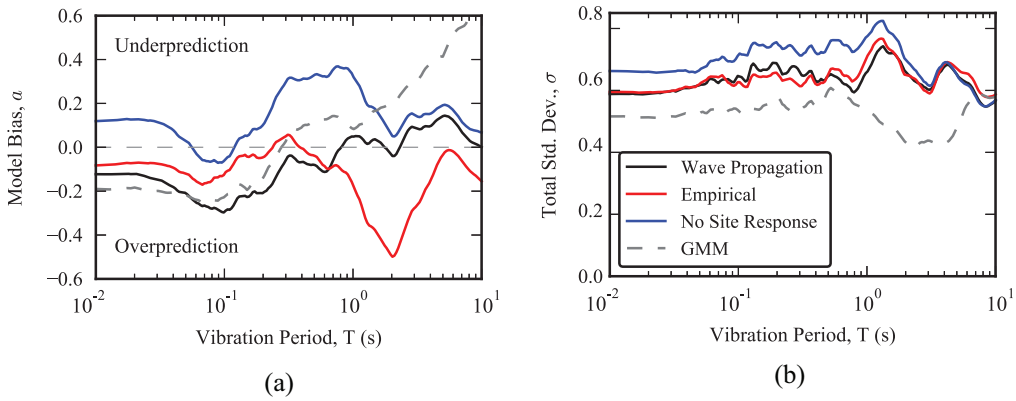

Figure 5. (a) Systematic model bias, a, and (b) total uncertainty, σ, for all events and sites considered.

arrivals not visible in observations. These late arrivals may be the cause of the large over estimation of long period energy seen in response spectra (Figure 4b).

Systematic prediction residuals

Response spectra are computed for observed ground motions and all three simulation approaches discussed in section "Methodology." The partitioned residuals are then computed from the response spectra of all events at every site via Equations 1 and 2. The following subsections compare and contrast the computed residuals from the three simulation types.

Model systematic bias and total uncertainty for all events and sites considered

Figure 5 illustrates the systematic model bias, a (Figure 5a), and the total standard deviation, σ (Figure 5b), for all 20 sites and 11 earthquakes considered as a function of response spectral vibration period for all three analysis methods. Results from prediction via empirical GMM are not discussed until section "Comparison with prediction from empirical GMM." Three average trends are identified in the results shown in Figure 5a: (1) For periods between approximately $T = 0.2 - 2\ s$, consideration of site effects using both the empirical and wave propagation methods results in reduced bias (i.e. residuals closer to zero) relative to the reference viscoelastic simulations which ignore site effects and grossly under-predict spectral accelerations. (2) The empirical (V_{S30}-based) approach significantly over-amplifies the long periods (i.e. approximately 1–5 s) and the wave propagation method performs better in this period range, and (3) the empirical (V_{S30}-based) method results in slightly lower bias than the wave propagation approach at $T<0.2\ s$ for which the wave propagation method over-predicts the ground motion. The subsequent three paragraphs discuss these trends in greater detail.

The first trend noted above is relatively self-evident. The significant underprediction by reference viscoelastic simulations without site response occurs near the range of profile periods for the sites (i.e. $T_1^* = 0.15 - 0.77$ s), at which large amplification occurs from near-surface soil response. The reference viscoelastic simulation neglects site effects and therefore fails to model this large amplification at the profile period.

The second trend noted above, over amplification by the empirical V_{S30}-based approach at $T = 1 - 5$ s, suggests that long period site effects are already being explicitly captured in the LF component of the ground motion simulations such that the empirical modification is, to some extent, effectively "double counting" the amplification. This result was also observed by Lee et al. (2020) using the same simulation methodology, albeit without wave propagation site response, on a data set of 145 $M_W 3.5 - 5$ earthquakes in the same region. As previously noted, site amplification factors with truncation of long period amplification, as recommended by Graves and Pitarka (2010) (see Figure 3a), are intended to account for long period site effects when low-resolution velocity models are used that do not explicitly model these effects. However, the simulations used in this study are derived from a high-resolution Canterbury velocity model (Lee et al., 2017a) which explicitly models the basin, hence suggesting that the period range over which the site amplification function is heuristically truncated needs to be revised. In addition, the site amplification model from Campbell and Bozorgnia (2014) was developed primarily from California data, and therefore may not be appropriate for use in Christchurch.

Finally, regarding the third trend of overprediction of short period ground motion amplitudes, it is evident that the reference viscoelastic simulation (i.e. blue line in Figure 5a), which was used as an input motion for the wave propagation analysis, already overpredicts the observed ground motion at $T \approx 0.1\ s$ (relative to observed ground motions at $V_{S30} < 500$ m/s sites). This implies that periods close to 0.1 seconds would likely be further over-predicted for sites with near-surface shear wave velocities of less than 500 m/s when site effects are considered. In addition, the 1D wave propagation based site response analysis may not properly attenuate HFs which leads to excessive site amplification. Other studies have found that 1D wave propagation analysis, which typically lacks heterogeneities present in natural soil deposits that scatter and attenuate HF waves, can "underdamp" these frequencies (e.g. Afshari and Stewart, 2017).

Figure 5b shows that considering site effects via both the wave propagation and empirical methods reduces total uncertainty, σ, for $T < 2$ s relative to ignoring site effects in the case of viscoelastic simulations. As discussed in Supplemental Appendix B, the reduction in uncertainty for $T < 1$ is attributed primarily to a reduction in between-event uncertainty, τ. Both site response methods have comparable uncertainty across the full period range. Reasons for this are discussed with regard to event- and site-specific uncertainty in Supplemental Appendix B and section "Site-to-site, $\delta S2S_s$, and within-event, δW_{es}, residuals," respectively.

Site-to-site, $\delta S2S_s$, and within-event, δW_{es}, residuals

The site-to-site residual, $\delta S2S_s$ (Equation 2), represents the average difference between observed and predicted site amplification at a given site. Figure 6 plots the site-to-site residuals for the wave propagation analysis, and the site-to-site and within-event single-station standard deviations, ϕ_{S2S} and ϕ_{SS}, respectively, for all three methods. The residuals for the viscoelastic reference simulations and simulations with empirical site response are plotted in Figure E.1 of Supplemental Appendix E. The site-to-site residuals (Figure 6a) are color-coded by the site V_{S30}, which illustrates a dependence in the residual on V_{S30} at approximately $T = 0.5 - 3\ s$. Generally, the stiffest sites are the most overpredicted, the softest sites are the most underpredicted, and intermediately stiff sites fall close to zero residual in this period range. This trend is even more notable for the $\delta S2S_s$ residuals of viscoelastic reference simulations that neglect shallow site response, which is reasonable as one would

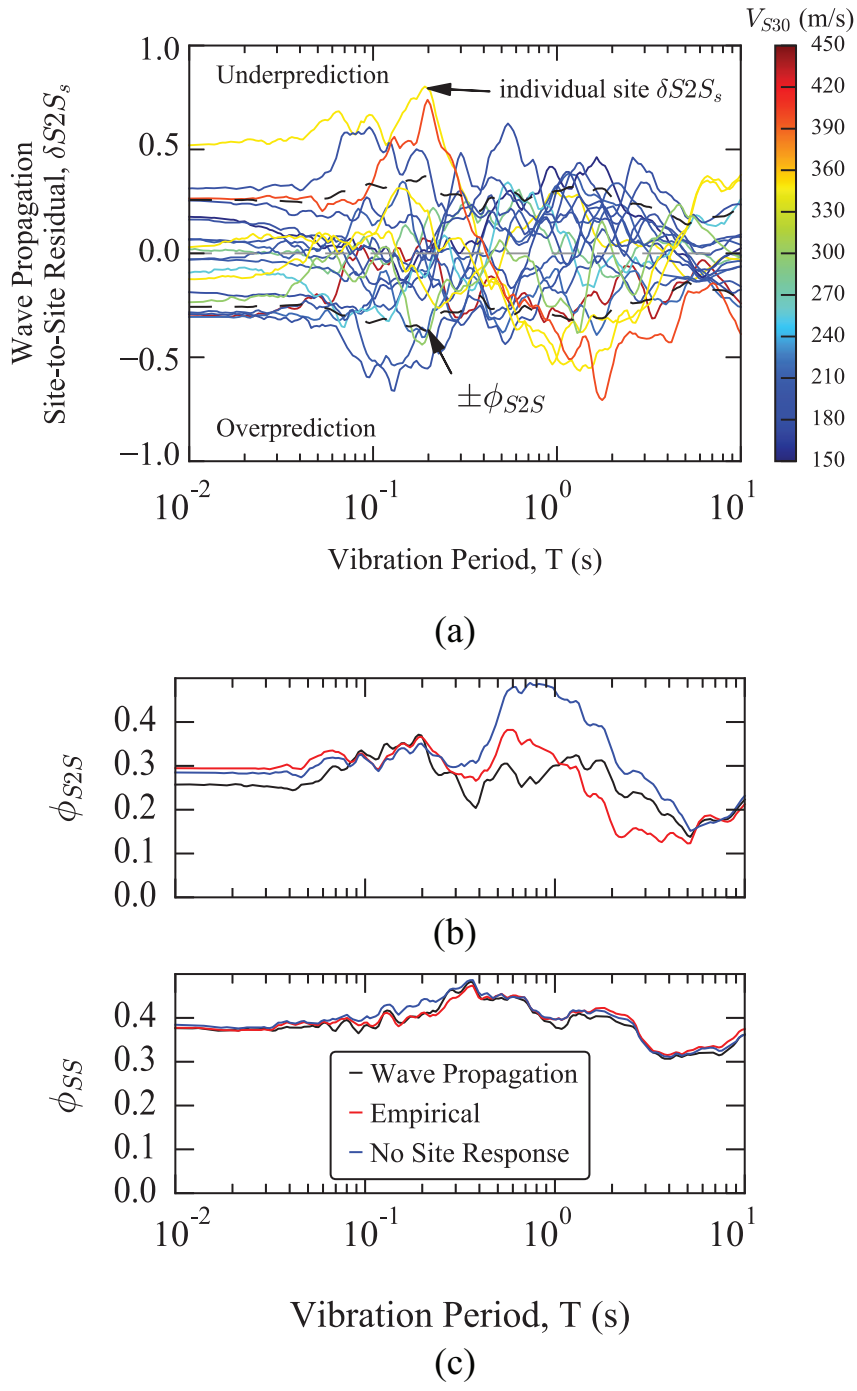

Figure 6. (a) Site-to-site residuals from wave propagation site response analysis for all 20 sites with lines colored by V_{S30}, and (b) site-to-site standard deviation, ϕ_{S2S}, and (c) within-event single-station standard deviation, ϕ_{SS}, respectively, for wave propagation, empirical, and reference viscoelastic (i.e. no site response) simulated ground motions.

expect the softest sites, with the strongest site amplification, to be even more under-predicted when site effects are neglected. Two conclusions can be drawn from the fact that this trend is still visible in the wave propagation site response results: (1) Although the wave propagation site response analysis greatly reduces the large under-prediction at soft sites by modeling site response, the modeling assumptions mean the analysis does not fully capture the actual site amplification, resulting generally in a slight under-prediction (Figure 6a), or (2) the large majority of stiffer sites lie in the same region to the west of Christchurch in the Canterbury plains (Figure 2). This overprediction at moderate to long periods could alternatively be a regional effect caused by the 3D velocity model (i.e. path) for this region. Because the mean of all $\delta S2S_s$ must be zero, this regional over-prediction would cause an apparent under-prediction in the remaining sites, particularly for softer sites at which the observed site amplification is greater.

Theoretically, by perfectly modeling the site response, each individual site-to-site residual ($\delta S2S_s$) could be reduced to zero. The departure of $\delta S2S_s$ from zero is therefore indicative of both physics that is not adequately modeled in the site response analysis, and uncertainty in the geotechnical and geophysical site characterization. In addition, because $\delta S2S_s$ represents the observed-to-simulated differences in site amplification, it is highly dependent on the input motion obtained from the regional ground motion simulation as nonlinear site response is greatly influenced by the amplitude and frequency content of the ground motion. Therefore, imprecision in the input motion will inevitably manifest as non-zero $\delta S2S_s$ residuals. While $\delta S2S_s$ is non-zero for the simulations with site effects modeling, it is evident from Figure 6b that a reduction in uncertainty is realized when site effects are considered.

Figure 6b shows that consideration of site effects via both the empirical and the wave propagation methods substantially decreases the site-to-site uncertainty, ϕ_{S2S}, for $T \approx 0.3 - 5.0\ s$. This implies that the site amplification is predicted with less uncertainty when near-surface site effects are considered in physics-based ground motion simulation. Explicitly modeling site response via wave propagation reduces site-to-site uncertainty compared with the V_{S30}-based empirical method at $T = 0.2 - 1\ s$, which is approximately the range of profile periods for the SMS considered (i.e. $T_1^* = 0.15 - 0.77s$; as defined in Table A.2 of Supplemental Appendix A). For $T = 1 - 5\ s$, where the 1D wave propagation site response analysis has little influence on spectral accelerations for these sites, the V_{S30}-based empirical site amplification has slightly lower site-to-site standard deviation than the wave propagation method. One would expect that the site response approach which uses both significantly more information on soil type and stratigraphy, and also more comprehensive physics (i.e. the wave propagation analysis), would potentially result in less uncertainty in the site amplification. The fact that there is no appreciable difference in uncertainty for much of the period range between the two site response approaches suggests that, as alluded to previously, there is both uncertainty in the input motion, and potentially the assumptions in the 1D total stress site response analysis (including the determination of modeling parameters) is leading to significant imprecision. The total uncertainty is contributed to by both of these factors and further work is needed to untangle them, and thus isolate their relative contributions (this is discussed further in Supplemental Appendix C).

As shown in Figure 6c, the within-event single station standard deviation (ϕ_{SS}) is practically the same for all three analyses over the entire period range. ϕ_{SS} represents the apparent aleatory variability that is not systematically modeled by the physics used in these models, and includes effects from the source, path, and site. A reduction in ϕ_{S2S} with no change in ϕ_{SS} suggests that the mean site amplification is predicted with more accuracy

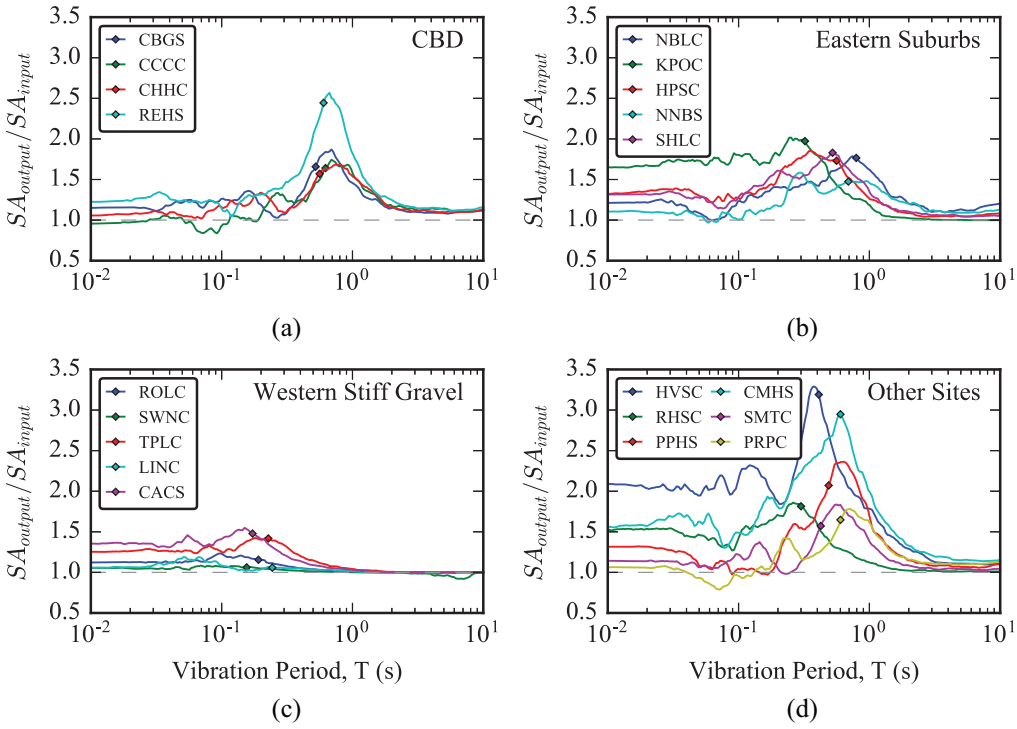

Figure 7. Spectral acceleration amplification functions (i.e. the ratio of computed ground surface motion over the input motion) from wave propagation site response analyses for (a) CBD, (b) Eastern Suburbs, (c) Western Stiff Gravel sites, and (d) Other Sites. The small diamonds indicate the small-strain, pressure-independent profile period (T_1^*) for each site.

when site response is explicitly modeled, however, at any given station, the uncertainty in the modeled site amplification is the same for all methods or is masked by apparently random uncertainties in the source, path, and site. Single station uncertainty is discussed further in Section C.0.1 of Supplemental Appendix C.

Systematic residuals for individual sites

Figure 7 plots the average 1D wave propagation-based spectral acceleration amplification across the 11 events as a function of vibration period for each of the 20 profiles in Figure A.1 of Supplemental Appendix A. The amplification for an individual event is the ratio of the output motion at the ground surface to the input motion at the halfspace. It is apparent that sites REHS, HVSC, and CMHS have the largest average amplification, with amplification factors exceeding 2.5 at the profile period, while the western stiff sites profiles generate little amplification. The diamond on each curve indicates the profile period (i.e. T_1^*) as defined in section "Christchurch strong motion stations considered."

To illustrate how the level of site amplification is manifested in the systematic residuals of each site, Figure 8 plots the systematic residual (i.e. $a+\delta S2S$) from all three analysis methods for four sites. Figure 8a shows the results for HVSC, which consistently produced exceptionally strong ground shaking throughout the Canterbury Earthquake Sequence (Bradley, 2015; Jeong and Bradley, 2017a). This is evident from the large underprediction at $T<1$ *s* when site

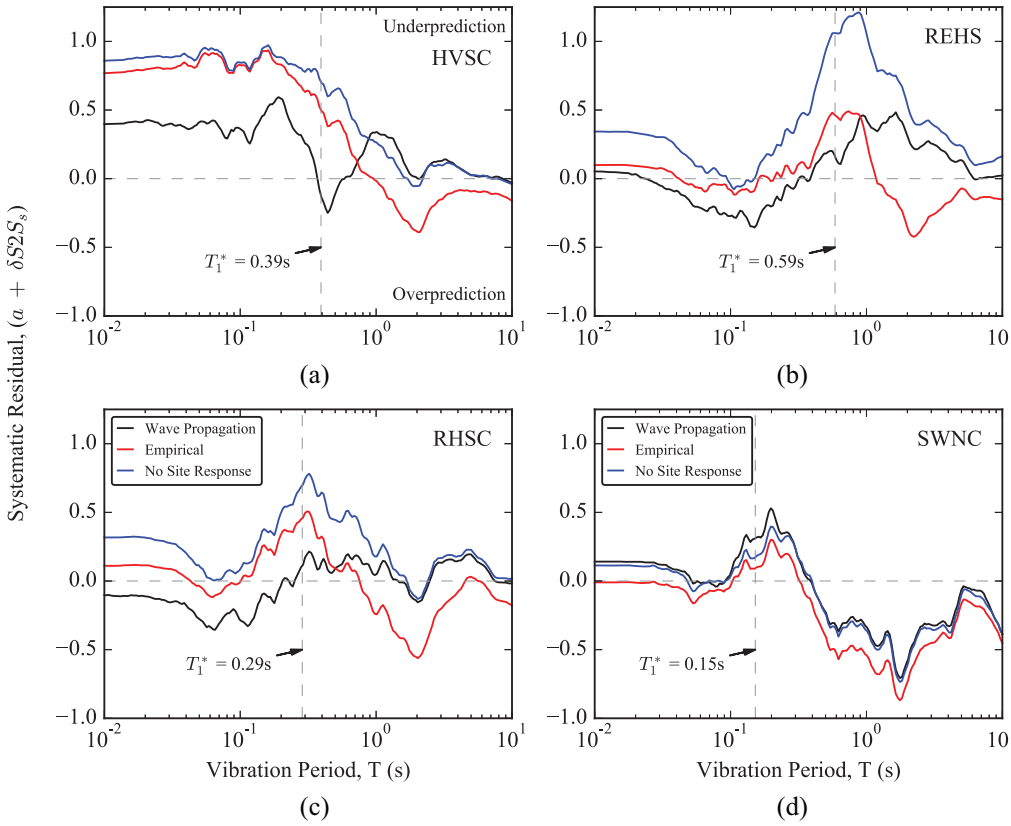

Figure 8. Comparison of systematic effect (i.e. $a + \delta S2S$) from three analysis methods for four sites: (a) HVSC, (b) RHSC, (c) REHS, and (d) SWNC.

effects are not considered (i.e. the reference viscoelastic simulations). The empirical V_{S30}-based amplification does not capture the strong site response and still severely underpredicts at short periods. The wave propagation site response analysis performs significantly better in this period range as a result of significant amplification being predicted (as shown in spectral amplification function of Figure 7d). Jeong and Bradley (2017a) found that this strong amplification can be attributed to 1D site effects from a large near-surface impedance contrast, and 2D/3D shallow basin response (Jeong and Bradley, 2017b). Since non-1D site response is not modeled in this study, further reduction in the systematic residual in Figure 8a would be possible using more comprehensive site effects modeling. It is also important to note that the 1D wave propagation method actually results in a slight overprediction due to the large amplification at T_1^* and that this could be improved by a more complex site response model that yields amplification over a broader period range.

Figure 7a shows that REHS (a soft peat soil site; Figure 2) systematically produces large site amplification and strong ground motions. The systematic residual for REHS in Figure 8b illustrates that the reference viscoelastic simulation greatly underpredicts spectral accelerations at the profile period ($T_1^* \sim 0.6$ s). The V_{S30}-based method does not fully capture the level of site amplification, and still results in substantial under-prediction at T_1^*. The wave propagation approach is better able to capture the strong amplification at the profile period and greatly reduces the systematic residual for this site.

As shown in Figure 8c, RHSC is yet another site at which the wave propagation site response analysis better predicts site amplification at the profile period. This site also demonstrates the overpredicting bias at short periods from the wave propagation analysis that is shown Figure 5 and discussed in section "Model systematic bias and total uncertainty for all events and sites considered" (i.e. trend (3)), which is likely a result of overprediction in the HF component of the reference simulations.

Finally, Figure 8d illustrates that at SWNC (a Western Stiff Gravel site; see Figure A.1 in Supplemental Appendix A) site response is negligible and therefore, all three analysis methods result in similar residuals. This trend is typical of all the Western Stiff Gravel sites. The large overprediction at $T = 0.5 - 3.0\ s$, which is discussed in detail in section "Site-to-site, $\delta S2S_s$, and within-event, δW_{es}, residuals," is also typical of these stiff gravel sites.

While the 1D wave propagation site response analysis is better able capture the large site amplification at the profile period for these sites, accurately predicting the precise amount of amplification at the profile period and at other periods is more challenging. The features presented in Figure 8 are further discussed with respect to all sites in Supplemental Appendix C. The systematic residual from all three analysis methods are plotted for every site in Figure E.2 of Supplemental Appendix E.

Figure C.1 in Supplemental Appendix C plots the systematic residual for all sites divided into groups (as in Figure 2) for both wave propagation and empirical methods. It highlights the trends in bias that are discussed in section "Model systematic bias and total uncertainty for all events and sites considered." Figure C.2 in Supplemental Appendix C directly compares the systematic residual at the profile period from empirical and wave propagation methods. The results indicate that for approximately 15% of sites, the wave propagation method greatly reduces the systematic residual. These sites are generally softer soil sites or sites with a large impedance contrast near the ground surface.

Comparison of observed and simulated response at nearby sites. This section compares the ground surface response of nearby sites within a group from both observed and simulated ground motions to examine whether the site response methods can capture local variability in ground motion that is presumably attributed only to near-surface site effects. Because the sites in the region considered here (i.e. CBD sites) are spatially close, this depiction of the data assumes that the incident ground motion below near-surface soils are practically similar. Spectral ratios are computed at every site and for every event as the ratio of the surface response spectrum for each site (i.e. $SA_{e,s}$) to the geometric mean response spectrum for the full group of sites (i.e. $SA_{e,mean}$). At every site, the geometric mean spectral ratio is then computed across all 11 events. This computation is expressed in equation form in Equations 4 and 5. The average spectral acceleration for an event, e, across all four sites in the CBD group (i.e. $N_{sites} = 4$) is computed as

$$SA_{e,mean} = \exp\left[\frac{1}{N_{sites}}\sum_{s=1}^{N_{sites}} \ln(SA_{e,s})\right] \tag{4}$$

At each site, s, the ratio of spectral acceleration at that site to the average spectral acceleration for the group is computed for all events. The average ratio across all 11 events (i.e. $N_{events} = 11$) is expressed as

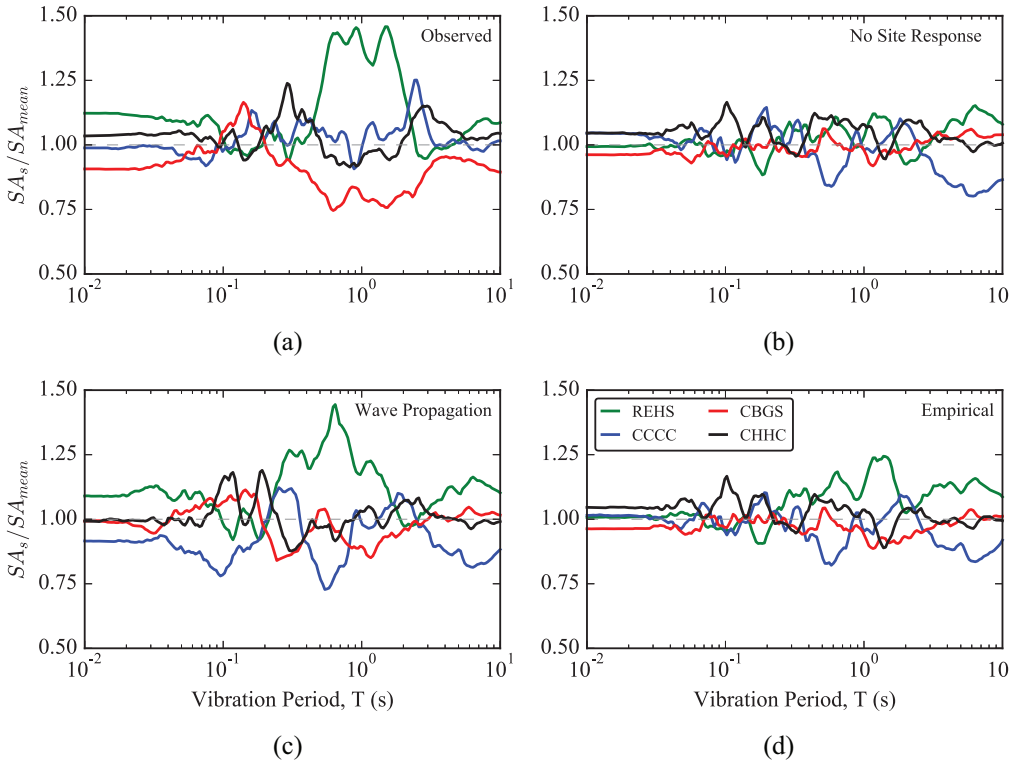

Figure 9. Response spectral ratios for sites within the Christchurch CBD from (a) observed ground motions, (b) reference viscoelastic simulations without site effects, (c) simulations with wave propagation site response, and (d) simulations with empirical V_{S30}-based site response. The spectral ratio corresponds to the mean ratio for all 11 events where the ratio for an individual ground motion is the spectral acceleration for a given site over the mean spectral acceleration from all sites in the group.

$$\frac{SA_s}{SA_{mean}} = \exp\left[\frac{1}{N_{events}}\sum_{e=1}^{N_{events}} \ln\left(\frac{SA_{e,s}}{SA_{e,mean}}\right)\right] \tag{5}$$

The advantage of using this type of metric versus others examined thus far is that it does not require assuming that the simulated incident ground motion below sites is consistent with observed ground motions. Figure 9 plots these spectral ratios for the CBD group from (a) observed ground motions, (b) simulated ground motions that neglect site effects, and those that model site effects via (c) wave propagation and (d) empirical V_{S30}-based site response. The observed ground motion ratios clearly illustrate strong amplification in the REHS ground motion relative to the other sites at periods $T = 0.5 - 2\ s$, as well as weaker shaking in this period range for Christchurch Botanic Gardens (CBGS). REHS is the softest of all 20 sites with the lowest V_{S30} (i.e. 155 m/s), as it has approximately 9 m of peat and soft silt below the ground surface (Wotherspoon et al., 2014). Other studies have also identified REHS as a site of exceptionally large site amplification (Bradley, 2015; Bradley et al., 2015).

As expected, because the distance between the sites is less than 2.5 km, the reference viscoelastic simulations with no site effects are similar across all CBD sites (Figure 9b). On

the contrary, the wave propagation site response analysis does a reasonably good job of capturing many of the relative differences in observed ground motions between sites (Figure 9c). Most notably, the wave propagation method captures the strong amplification near the profile period of REHS, although not to the full extent across the entire period range (i.e. $T = 0.5 - 2\ s$). At short periods, the below average and above average amplitudes at Christchurch College (CCCC) and REHS, respectively, are also captured by the models. In addition, the below average amplitudes at $T \approx 0.2 - 3\ s$ at CBGS are also seen in the wave propagation analysis. Some of the features that are inconsistent between the observed ratios and the wave propagation ratios can be attributed to the reference viscoelastic simulation (i.e. imprecision in the input motion) such as the strong relative deamplification in CCCC at about $T = 0.6\ s$, again illustrating that imprecision in the input motion will manifest as unfavorable bias in the computation of residuals.

Unlike the wave propagation method, the empirical V_{S30}-based method (Figure 9d) fails to capture all of the aforementioned trends in ground motions at nearby sites. This is most evident in the REHS ratios at which the relative amplification from this method is not nearly as large or broad as the observations. This exercise reiterates the significance of explicitly modeling site response for sites that are soft and/or exhibit strong site amplification as is discussed further in Supplemental Appendix C, but elucidates the difficulty in accurately predicting the precise amplitudes and frequency-dependence of ground amplification.

Comparison with prediction from empirical GMM

Until now, focus has been on the use of simulated viscoelastic "input" and alternative representations of surficial site response. In order to highlight the merit in this work presented to date, it is critical to benchmark results from these alternative physics-based ground motion simulations to conventional empirical GMMs, which are the current standard of practice for ground motion prediction. For the purpose of illustrative comparison, predicted response spectra were computed for all events and sites considered using the Bradley (2013) New Zealand-specific GMM, and residuals computed and partitioned according to Equations 1 to 3. Figure 5 plots the systematic model bias and total standard deviation for all events and sites from the three physics-based ground motion simulation methodologies, and the empirical GMM which also utilizes V_{S30}-based site amplification (from Chiou and Youngs, 2008).

In examining Figure 5a, no notable differences in the magnitude of bias are observed for $T<1\ s$. For $T>1\ s$, the bias in the GMM prediction increases substantially with increasing period, such that the GMM greatly underpredicts the long period intensity and the bias is significantly greater than that from physics-based simulations for $T>5\ s$. Such long period bias has also been noted by Van Houtte (2017). Even for $T>1\ s$, the wave propagation method has substantially lower bias than the GMM.

In Figure 5b, the total standard deviations show slightly less uncertainty for the GMM at $T<1\ s$, and moderately less uncertainty for $T = 1 - 5\ s$. For $T>5\ s$, the empirical GMM predicts ground motion with similar uncertainty as the physics-based approaches. Figure D.1 in the Supplemental Appendix D compares the components of standard deviation from all analysis methods. Figure D.1 in Supplemental Appendix D demonstrates that it is the between-event uncertainty, τ, that results in lower σ for $T = 1 - 5\ s$, and the site-to-site uncertainty, ϕ_{S2S} that results in higher σ for $T>5\ s$ from the GMM compared with the physics-based methods. Considering both the magnitude of bias and uncertainty, it can be concluded that for $T<5\ s$ the physics-based simulation and empirical GMM

methods predict ground motion with comparable performance while for $T>5\,s$ the physics-based methods performs significantly better.

All components of standard deviation from this study are also compared with previously published values from empirical prediction models in Supplemental Appendix D. Figure D.2 in Supplemental Appendix D again shows that these physics-based simulation methods can predict ground motion with comparable uncertainty as empirical GMMs.

Conclusion

This study compares and contrasts alternative approaches to modeling site response in physics-based ground motion simulations, and specifically highlights the benefits and hindrances of using a physics-based wave propagation site response methodology as opposed to the standard-of-practice empirical V_{S30}-based approach. In terms of the overall model bias across all events and sites considered, three notable observations are made: (1) Over a wide period range, consideration of site effects using both the empirical and wave propagation methods results in reduced bias (i.e. residuals closer to zero) relative to the reference viscoelastic simulations which ignore site effects and grossly under-predict spectral accelerations, (2) the V_{S30}-based approach significantly over-amplifies long period ground motions and the wave propagation method performs better in this period range, suggesting that the LF component of the ground motion simulation is capturing deep site effects reasonably well already, leading to a "double counting" of amplification, and (3) the empirical V_{S30}-based method performs slightly better than the wave propagation approach at short periods for which the wave propagation method overpredicts ground motions; This is also exacerbated by an over-prediction from the HF component of the simulation, as seen from the viscoelastic reference prediction for a reference shear wave velocity of 500 m/s. The total standard deviation is reduced for $T<2$ s when site effects are considered, however, there is no notable difference in σ between the wave propagation and empirical site response methods. The site-to-site uncertainty, which reflects uncertainty in site amplification, is also greatly reduced at approximately $T = 0.3 - 5$ s by modeling nonlinear site effects. Explicit modeling of site response via wave propagation results in even greater reduction in site-to-site uncertainty near the profile periods of the SMSs considered (i.e. $T = 0.2 - 1$ s).

While the systematic residual in ground motion prediction at the profile periods from the physics-based wave propagation and empirical V_{S30}-based methods are comparable for the majority of sites, significant improvements are realized in some instances with the wave propagation method for very soft sites or sites that exhibit exceptionally large site response. For these sites, the empirical V_{S30}-based site amplification fails to capture the large amplification and greatly under-predicts. Comparisons of average amplifications from nearby sites indicates that the wave propagation method is better able to model relative trends in site specific shallow ground response.

Investigation into systematic residuals and within-event single-station standard deviations for stiff gravel sites that have negligible impedance-based site response suggests that there is imprecision in the reference viscoelastic simulated motions which are used as input to the site response analyses. This likely limits the amount of improvement that can be realized by explicitly modeling nonlinear site effects.

Perhaps of utmost importance, these physics-based ground motion simulations with nonlinear site effects (especially the wave propagation method), can generally predict

spectral accelerations with comparable bias and uncertainty, and with significantly lower bias at $T>5\ s$ relative to empirical GMMs. This suggests that these simulated ground motions are equally as appropriate as conventional empirical GMMs for use in geotechnical and structural response history analysis. In addition, because of the physics-based nature of wave propagation site response coupled with physics-based ground motion simulations, there is significant room for improvement. This could be via improvement of the simulations themselves (i.e. refinement of regional velocity models, and development and adoption of improved methodologies), or the site characterization and site response analysis.

Data and resources

Observed ground motions used for computing prediction residuals were downloaded from the GeoNet file transfer protocol (ftp://ftp.geonet.org.nz/strong/). The physics-based ground motion simulations were obtained from Hoby Razafindrakoto et al. (2016). The simulations for the 2010 Darfield and 2011 Christchurch earthquakes are available on SeisFinder (https://quakecoresoft.canterbury.ac.nz/seisfinder/).

Figures 1 and 2 were generated using Generic Mapping Tools (http://gmt.soest.hawaii.edu/), and the remaining figures were generated in Python (https://www.python.org/) and Matplotlib (https://matplotlib.org/).

Acknowledgments

The authors thank Hoby Razafindrakoto for providing the simulated ground motions used in this study; Christopher McGann, Liam Wotherspoon, Seokho Jeong, Jim Kaklamanos, Kevin Foster, and Karim Tarbali for their technical and editorial support; and Viktor Polak for generating Figures 1 and 2.

Declaration of conflicting interests

The author(s) declared no potential conflicts of interest with respect to the research, authorship, and/or publication of this article.

Funding

The author(s) disclosed receipt of the following financial support for the research, authorship, and/or publication of this article: This work was financially supported by the University of Canterbury, and QuakeCoRE: The NZ Center for Earthquake Resilience via the UC and QuakeCoRE PhD Scholarships. This is QuakeCoRE publication number 0371.

Supplemental material

Supplemental material for this article is available online.

References

Afshari K and Stewart JP (2017) Small-strain damping for ground response analysis as used in non-ergodic hazard analysis —Lessons from California recordings. Technical Report, UCLA, Los Angeles, CA. Available at: https://escholarship.org/uc/item/7cx9x9mc

Al Atik L, Abrahamson N, Bommer JJ, et al. (2010) The variability of ground-motion prediction models and its components. *Seismological Research Letters* 81: 794–801.

Bates D, Mächler M, Bolker B, et al. (2015) Fitting linear mixed-effects models using lme4. *Journal of Statistical Software* 67: 1–48.

Beavan J, Fielding E, Motagh M, et al. (2011) Fault location and slip distribution of the 22 February 2011 Mw 6.2 Christchurch, New Zealand, earthquake from geodetic data. *Seismological Research Letters* 82: 789–799.

Beavan J, Motagh M, Fielding EJ, et al. (2012) Fault slip models of the 2010–2011 Canterbury, New Zealand, earthquakes from geodetic data and observations of postseismic ground deformation. *New Zealand Journal of Geology and Geophysics* 55: 207–221.

Bielak J, Loukakis K, Hisada Y, et al. (2003) Domain reduction method for three-dimensional earthquake modeling in localized regions, part I: Theory. *Bulletin of the Seismological Society of America* 93: 817–824.

Bora SS, Scherbaum F, Kuehn N, et al. (2016) On the relationship between Fourier and response spectra: Implications for the adjustment of empirical ground-motion prediction equations (GMPEs). *Bulletin of the New Zealand Society for Earthquake Engineering* 106: 1235–1253.

Bradley BA (2013) A New Zealand-specific pseudospectral acceleration ground-motion prediction equation for active shallow crustal earthquakes based on foreign models. *Bulletin of the Seismological Society of America* 103: 1801–1822.

Bradley BA (2015) Systematic ground motion observations in the Canterbury earthquakes and region-specific non-ergodic empirical ground motion modeling. *Earthquake Spectra* 31: 1735–1761.

Bradley BA, Jeong S and Razafindrakoto H (2015) Strong ground motions from the 2010-2011 Canterbury earthquakes and the predictive capability of empirical and physics-based simulation models. In: *Proceedings of the tenth Pacific conference on earthquake engineering*, Sydney, NSW, Australia, 6–8 November.

Bradley BA, Razafindrakoto HNT and Polak V (2017) Ground-motion observations from the 14 November 2016 Mw 7.8 Kaikora, New Zealand earthquake and insights from broadband simulations. *Seismological Research Letters* 88: 740–756.

Brown L, Beetham R, Paterson B, et al. (1995) Geology of Christchurch, New Zealand. *Environmental & Engineering Geoscience* 1: 427–488.

Campbell KW and Bozorgnia Y (2014) NGA-West2 ground motion model for the average horizontal component of PGA, PGV, and 5% damped linear acceleration response spectra. *Earthquake Spectra* 30: 1087–1115.

Chiou BSJ and Youngs RR (2008) An NGA model for the average horizontal component of peak ground motion and response spectra. *Earthquake Spectra* 24: 173–215.

Cubrinovski M, Bray JD, Taylor M, et al. (2011) Soil liquefaction effects in the central business district during the February 2011 Christchurch earthquake. *Seismological Research Letters* 82: 893–904.

Cubrinovski M, Winkley A, Haskell J, et al. (2014) Spreading-induced damage to short-span bridges in Christchurch, New Zealand. *Earthquake Spectra* 30: 57–83.

Deschenes M, Wood C, Wotherspoon L, et al. (2018) Development of deep shear wave velocity profiles in the Canterbury Plains, New Zealand. *Earthquake Spectra* 34, 1065–1089.

Graves R and Pitarka A (2010) Broadband ground-motion simulation using a hybrid approach. *Bulletin of the Seismological Society of America* 100: 2095–2123.

Graves R and Pitarka A (2015) Refinements to the graves and Pitarka (2010) broadband ground-motion simulation method. *Seismological Research Letters* 86: 75–80.

Hartzell S, Alena L, Frankel A, et al. (2002) Simulation of broadband ground motion including nonlinear soil effects for a magnitude 6.5 earthquake on the Seattle Fault, Seattle, Washington. *Bulletin of the Seismological Society of America* 92: 831–853.

Idriss IM and Boulanger RW (2008) *Soil Liquefaction During Earthquakes* (Monograph-12), Oakland, CA: Earthquake Engineering Research Insitute.

Jeong S and Bradley B (2017a) Amplification of strong ground motions at Heathcote Valley during the 2010-2011 Canterbury earthquakes: Observation and 1D site response analysis. *Soil Dynamics and Earthquake Engineering* 100: 345–356.

Jeong S and Bradley B (2017b) Amplification of strong ground motions at Heathcote Valley during the 2010-2011 Canterbury earthquakes: The role of 2D non-linear site response. *Bulletin of the Seismological Society of America* 107: 160389.

Kaklamanos J, Bradley BA, Thomson E, et al. (2013) Critical parameters affecting bias and variability in site-response analyses using KiK-net downhole array data. *Bulletin of the Seismological Society of America* 103: 1733–1749.

Kramer S (1996) *Geotechnical Earthquake Engineering*. Upper Saddle River, NJ: Prentice Hall.

Lee RL, Bradley BA, Ghisetti FC, et al. (2017a) Development of a 3D velocity model of the Canterbury, New Zealand, region for broadband ground-motion simulation. *Bulletin of the Seismological Society of America* 107: 2131–2150.

Lee RL, Bradley BA and McGann CR (2017b) 3D models of quaternary-aged sedimentary successions within the Canterbury, New Zealand region. *New Zealand Journal of Geology and Geophysics* 60: 320–340.

Lee RL, Bradley BA, Stafford PJ, et al. (2020) Hybrid broadband ground motion simulation validation of small magnitude earthquakes in Canterbury, New Zealand. *Earthquake Spectra* 36(2): 673–699.

McGann CR, Bradley B and Cubrinovski M (2017) Development of regional VS30 model and typical Vs profiles for Christchurch, New Zealand from CPT data and region-specific CPT-Vs correlation. *Soil Dynamics and Earthquake Engineering* 95: 48–60.

McKenna, F (2011). OpenSees: A framework for earthquake engineering simulation. *Computing in Science and Engineering* 13: 58–66.

Quigley MC, Hughes MW, Bradley BA, et al. (2016) The 2010-2011 Canterbury earthquake sequence: Environmental effects, seismic triggering thresholds, and geologic legacy. *Tectonophysics* 672/673: 228–274.

Razafindrakoto H and Bradley B (2016) YouTube video: 14 February 2016 Christchurch NZ earthquake (Mw5.8) simulation. https://www.youtube.com/watch?v = JtT_tT6NoEk

Razafindrakoto HNT, Bradley BA and Graves RW (2016) Broadband ground motion simulation of the 2010-2011 Canterbury earthquake sequence. In: *Proceedings of the 2016 New Zealand Society of earthquake engineering conference*, Christchurch, New Zealand, 1–3 April.

Razafindrakoto HNT, Bradley BA and Graves RW (2018) Broadband ground-motion simulations of the 2011 MW 6.2 Christchurch, New Zealand, earthquake. *Bulletin of the Seismological Society of America* 108: 2130–2147.

Régnier J, Bonilla LF, Bard PY, et al. (2016) Internal benchmark on numerical simulations for 1D nonlinear site response (PRENOLIN): Verification phase based on Canonical cases. *Bulletin of the Seismological Society of America* 106: 2112–2135.

Restrepo D, Taborda R and Bielak J (2012) *Three-dimensional nonlinear earthquake ground motion simulation in the Salt Lake basin using the Wasatch Front community velocity model*. Technical Report G10AP00077. Pittsburgh, PA: Computational Seismology Laboratory, Department of Civil and Environmental Engineering, Carnegie Mellon University, January 2012.

Robertson PK and Wride CE (1998) Evaluation of cyclic liquefaction potential using the cone penetration test. *Canadian Geotechnical Journal* 35: 442–459.

Roten D, Cui Y, Olsen L, et al. (2016) High-frequency nonlinear earthquake simulations on petascale heterogeneous supercomputers. In: *Proceedings of the 2016 conference for high performance computing, networking, storage and analysis*, Salt Lake City, UT, 13–18 November.

Roten D, Olsen K and Pechman J (2012) 3D simulations of M 7 earthquakes on the Wasatch Fault, Utah, part II: Broadband (0-10 Hz) ground motions and nonlinear soil behavior. *Bulletin of the Seismological Society of America* 102: 2008–2030.

Stewart JP, Afshari K and Goulet CA (2017) Non-ergodic site response in seismic hazard analysis. *Earthquake Spectra* 33: 1385–1414.

Stewart JP, Kwok AO, Hashash YMA, et al. (2008) *Benchmarking of nonlinear geotechnical ground response analysis procedures*. Technical Report PEER 2008/04, August. Berkeley, CA: Pacific Earthquake Engineering Research Center.

Taborda R and Bielak J (2013) Ground-motion simulations and validation of the 2008 Chino Hills, California, earthquake. *Bulletin of the Seismological Society of America* 103: 131–156.

Taborda R, Bielak J and Restrepo D (2012) Earthquake ground-motion simulation including nonlinear soil effects under idealized conditions with application to two case studies. *Seismological Research Letters* 83: 1047–1060.

Thompson EM, Baise LG, Kayen RE, et al. (2009) Impediments to predicting site response: Seismic property estimation and modeling simplifications. *Bulletin of the Seismological Society of America* 99: 2927–2949.

van Ballegooy S, Malan P, Lacrosse V, et al. (2014) Assessment of liquefaction-induced land damage for residential Christchurch. *Earthquake Spectra* 30: 31–55.

Van Houtte C (2017) Performance of response spectral models against New Zealand data. *Bulletin of the New Zealand Society for Earthquake Engineering* 250: 21–38.

Wotherspoon L, Orense R, Bradley B, et al. (2014) Geotechnical characterisation of Christchurch strong motion stations. Technical Report Earthquake Commission Report Project No. *12/629, Version 2*.0, October. Auckland, New Zealand: The University of Auckland.

Yang Z, Elgamal A and Parra E (2003) Computational model for cyclic mobility and associated shear deformation. *Journal of Geotechnical and Geoenvironmental Engineering: ASCE* 129: 1119–1127.

Yoshimura C, Bielak J, Hisada Y, et al. (2003) Domain reduction method for three-dimensional earthquake modeling in localized regions, part II: Verification and applications. *Bulletin of the Seismological Society of America* 93: 825–840.